

## Effect of Sutural Pattern on Shell Shape: A Case Study Including Two Ammonite Subfamilies from the Western India

Pinaki Roy

Department of Geology, Durgapur Government College, Durgapur, India.

### ABSTRACT

Shell morphology of ammonites and its connotation with ecological constraints has long been a matter of debate. The present study involves comparison of shell morphology with sutural complexity between *Eucycloceratin* and *Reineckeina* ammonites of Kutch and Jaisalmer from India. Statistically significant differences between fractal-dimensions ( $D_f$ ), whorl expansion rate of evolute and involute shells are interpreted. There is also a correlation between the flank's shape and complexity of suture. The planulate shells show highest  $D_f$  value and the lowest ones are found in whorl cross section with convex flanks. It may also be stated that sutural complexity is not the primary function to resist shell implosion and is thereby related to bathymetry.

**Keywords:** Ammonite, Suture, Shell-geometry, *Eucycloceratinae*, *Reineckeinae*, Western India.

### 1. Introduction

The present study has attempted to find out the relationship between the complexly frilled ammonoid suture patterns and their shell geometry. The complexity of ammonoid sutures is such that Euclidean geometry is unable to describe them properly [1]. The fractal dimension ( $D_f$ ) of the suture was measured in a more favorable manner using fractal analysis, which may serve as a morphometric descriptor of the complexity. Its value lies between 1 and 2 since a straight line has a Euclidean dimension of one and a curve's sinuosity can closely fill a plain, which provides an effective or fractal dimension approximately equivalent to two [1]. Thus, sutures with greater complexity have a  $D_f$  value that is closer to two. In the ammonite morpho-space,  $D_f$  values are mainly determined by structural (shell architecture) and ornamental factors (sculpture strength rather than density of ornamentation). Previous studies [2] have found little evidence to suggest that the complexity of sutures in Late Jurassic ammonites is largely determined by the bathymetry of epicontinental and epiocenic environments, with the highest values of  $D_f$  found in planulate shells and the lowest in whorl cross sections with convex flanks. The enigmatic complexity of ammonoid sutures has confounded researchers [3] for many years. Two primary queries are yet to be answered: Why did the sutures form such diverse patterns which were not correlated to the shell morphology, and why did these sutural patterns evolve so quickly compared to the limited range of shell shapes? Despite considerable effort, these questions remain largely unresolved. Different explanations have been proposed for the complexity of septal geometry in ammonites: according to functional morphological aspect, the frilled sutures increased buttressing, which strengthened the shell against implosion. This is allowed for respiration and transport of cameral liquid. The frills were a result of body attachment and muscle attachment, mantle tie-points, and interactive vaulting. The physical properties of this included viscous fingering in fluid interfaces during morphogenesis, as well as compression and decompression of a bladder due to the movability of a fleshy

membrane [4]. This can be related to accommodation space within the body chamber of ammonite-compressed shell needs more accommodation space, so complex sutures. Shell with convex flanks already has enough space for accommodating a bladder, so a simpler suture serves the



purpose in this case.

Fig. 1: *Reineckeia tyranniformis* from the subfamily *Reineckeinae* (Scale bar = 1 cm)

To testify the above hypothesis, two ammonite subfamilies have been chosen viz. *Reineckeinae* belonging to the family *Reineckeidae* (Fig. 1) and *Eucycloceratinae* belonging to the family *Sphaeroceratidae* (Fig. 2) from the Middle Jurassic of western India. Samples mainly have been collected from Kuldhara River section (Latitude = 26°48'74" N and Longitude = 70°48'1"E) in the Kuldhara Member of the Jaisalmer Formation, 16 km southwest of Jaisalmer, Rajasthan and near Bhakri village (Latitude = 23°22'34" N and Longitude = 69°36'29"E), which lies to the northwestern part

\*Corresponding author: pinakieroy@gmail.com

of the district town Bhuj, in Kutch, Gujarat. Both the ammonite subfamilies were widespread in their distribution in those two separate basins. Samples from two palaeobiogeographic distribution were taken to understand if there is any variability in ammonite morpho-space. Samples of three species from the subfamily Reineckeinae viz., *Reineckeia (Reineckeia) tyranniformis*, *Reineckeia (Loczyceras) turgida* and *Reineckeia (Loczyceras) reissi* and three species from the subfamily of Eucycloceratinae viz., *Idiocycloceras dubium*, *Idiocycloceras perisphinctoides* and *Nothocephalites paradoxus* have been considered within this present study. Those two groups of species show variability in their degree of whorl inflation (rate of increment of whorl width relative to whorl height) as well as degree of involution (degree of tightness of coiling of ammonite shell).



Fig. 2: *Nothocephalites paradoxus* from the subfamily Eucycloceratinae (Scale bar = 1 cm.)

## 2. Geological Setting of the study area

The basins of Jaisalmer and Kutch originated in response to the reactivation of ancient fracture zones, which was a part of the overall rifting history of the Gondwana super plate. The initiation of the rifting in the region was at the start of Permian and in general proceeded from north to south. The Bikaner-Nagaur and Jaisalmer areas of Western Rajasthan and Axial Belt, Kirthar-Sulaiman and Kohat-Potwar areas of Pakistan formed the already emerged Indian shield's north-western slopes which were bounded on the three sides by the basement ridges of the Aravalli-Delhi fold belt (NW-SE Aravallis in the southeast, Delhi-Sargodha ridge in the northeast and Delhi ridge in the south).

### 2.1 Kutch Basin

Due to recurrent transgression and regression processes, sedimentation began shortly after the Kutch Basin opened as an early rifting of Gondwana in the Middle Jurassic [5]. Bathonian to Middle Tithonian Jurassic rocks can be encountered in the Kutch Basin. Biswas [6] established a

litho-stratigraphic classification based on extensive mapping and lithofacies studies of the intra-rift sub-basins. The Kutch Mainland, the Pachham, and the Eastern Kutch litho-stratigraphic areas were distinguished. The Rann, a large salt flat, separated these settlements (see Fig. 3). The regional structure consists of three parallel anticlines that run northwest to southeast. North of the basin, in the middle anticline, the most developed Jurassic rocks can be found [7, 8]. As seen at the famous Callovian sequence locations of Jara, Jumara, Keera, and Jhura, these anticlines have undergone superimposition of folding, resulting in the characteristic interference pattern cropping up as topographical domes. The northern flanks of these domal formations are terminated by an east-west trending fault that was triggered by the intrusion of later Deccan Trap Volcanics. The Kutch Basin is divided into several distinct lithostratigraphic units, the most important of which are the Patcham, Chari, Katrol, and Bhuj Formations [9, 10]. Inliers of the younger Katrol Formation border the older Patcham and Chari Formations.

There are currently a number of important papers [11, 12] on the sedimentology and facies study of the region. The Chari Formation is comprising of shale, limestone, and sandstone heterolithic facies association that was deposited in a mid-shelf setting. Lower Callovian rocks in this Formation are dominated by shale-limestone (packstone/wackestone) alternations, whereas Middle Callovian rocks are made up of siliciclastics at their base. The present study relies on fossils acquired from the Bhakri sections of the Chari Formation.

### 2.2 Jaisalmer Basin

The Jaisalmer Basin is a pericratonic basin and represents mainly the westerly dipping eastern flank of the Indus Shelf. The existence of faults with strike-slip regime with its complimentary structural styles governing sedimentation history has been noticed in the basin [13]. The Jaisalmer Basin experienced its first sedimentation on igneous/metamorphic basement during Late Palaeozoic time which continued up till recently and sediments of huge thickness of the order of 10,000 m or so were deposited. Lithostratigraphically, the Jurassic sediments of the basin have been grouped into Lathi, Jaisalmer, Baisakhi and Bhadasar Formations in ascending order (Fig. 4) [14-18]. The thickness of individual formation ranges from 70 to 1000 m [14, 19]. Among these, the Jaisalmer Formation Ranges from Late Bajocian to Oxfordian age i.e., the Jurassic time. Lithostratigraphically, the Jaisalmer Formation has been divided, in ascending order, into the Hamira, Joyan, Fort, Badabag, Kuldhara and Jajiya Members [14, 20]. The Callovian-Oxfordian sediments of the Jaisalmer Formation, grouped into Kuldhara and Jajiya Members, are predominantly Carbonates deposited in the shoreface zone to off-shore transition zone above storm wave-base [21]. These are the best outcrops of the Callovian and Oxfordian sediments in the Jaisalmer Basin. The specimens of the present study have been collected from the Kuldhara Member of Jaisalmer Formation.

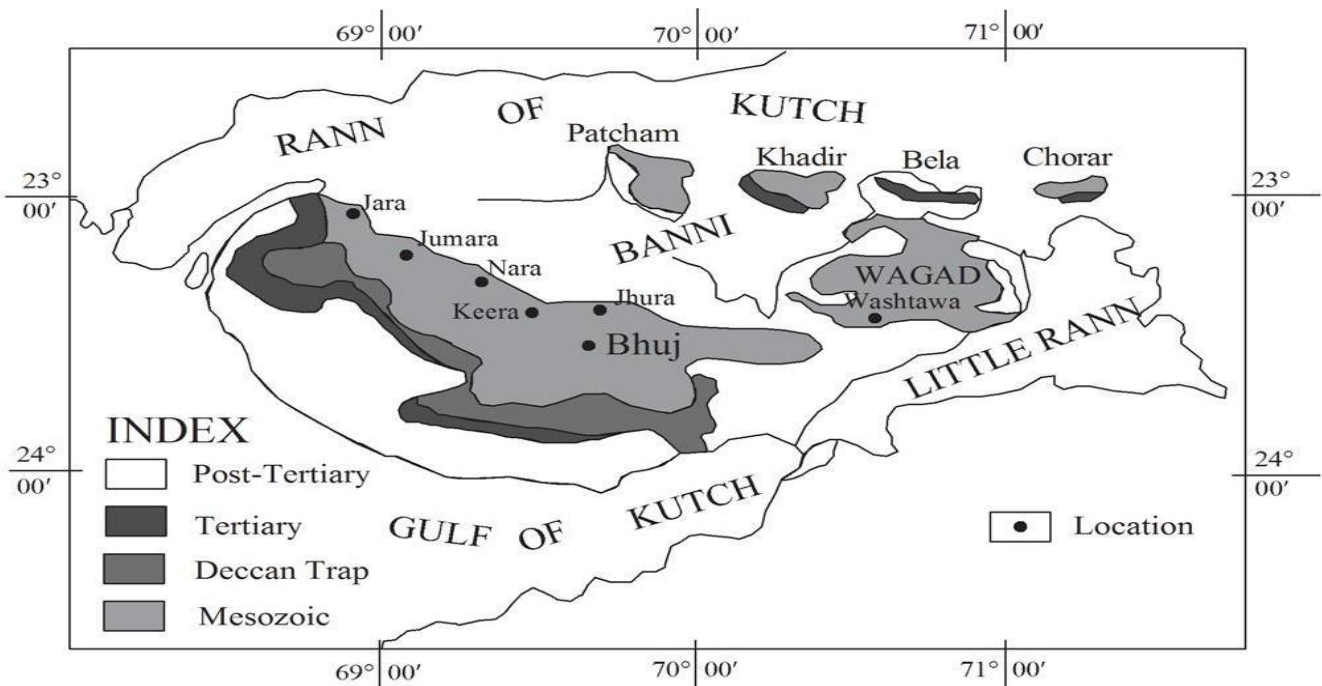


Fig. 3: Geological map of Kutch western India with the geographical locations of the study area.

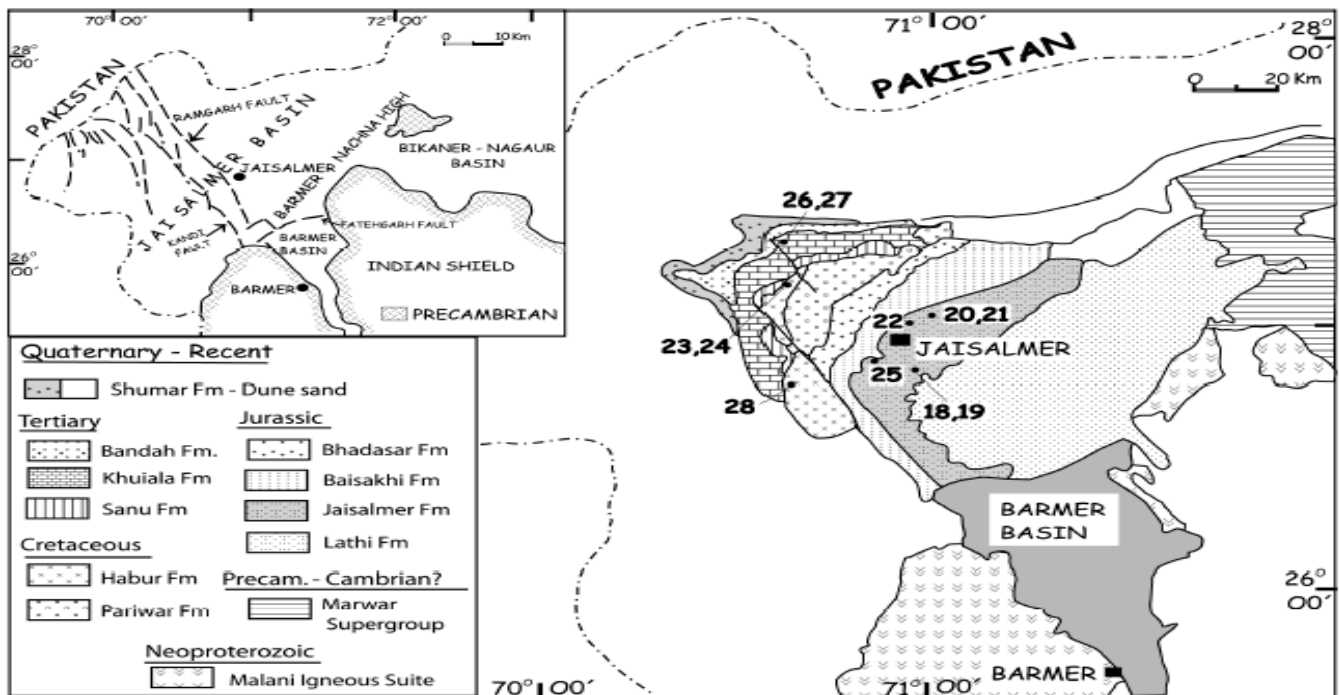


Fig. 4: Geological setting and location of the Jaisalmer basin.

### 3. Materials and Methods

The analyzed sutures were traced out from scaled photographs of actual specimens collected from the field. The dataset comprises 14 specimens and in each 3 sutures were analyzed, based on ontogeny. The specimens belong to 3 genera and 6 species.

The complexity of the sutures of these ammonites was analyzed based on their fractal dimension values. Two of the

most commonly used methods to determine the fractal dimension of ammonite sutures are the Richardson step-line division method [22, 23] and the box method. The Richardson analysis [2, 24, 25] determines how the length of a curve is correlated to the stride length of a divider, or the length of the ruler, used to measure it. As the length of the ruler or step size decreases, the lengths of the fractal curves increase, and a log-log graph of the length measurement vs. the corresponding strides will yield a straight line if the curve exhibits a truly

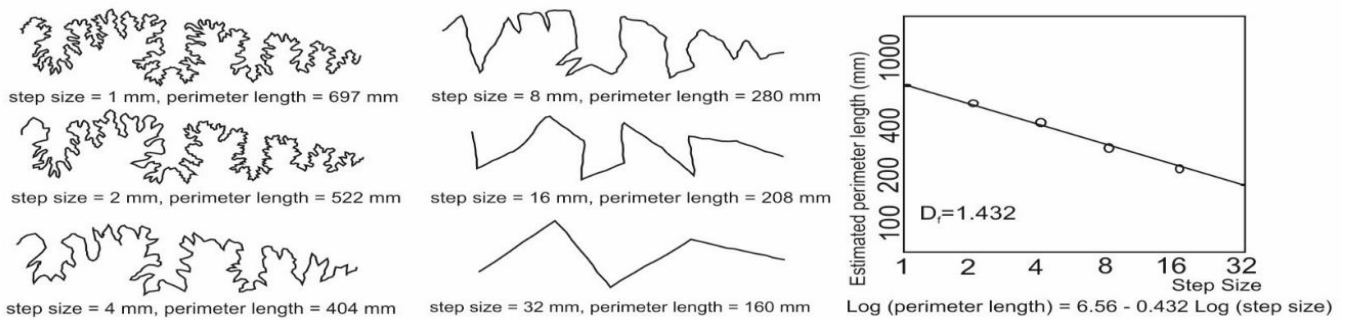


Fig. 5: Perimeter length measurement and estimation of the fractal-dimension (of) value of an ammonitic suture using the step-line method. The bi-variate graph shows how the perimeter estimated for the curve is inversely related to the length of the ruler.

fractal nature (Fig. 5). The fractal dimension value of the curve can be obtained from the following equation, which is adjusted by least-squares regression:

$$\text{Log (perimeter length)} = \text{Log}(k) + (1-D_f) \text{Log (step size)}$$

where  $k$  is the Y-intercept or length measurement for unit ruler length (step-size= 1).

The number of squared boxes of a given size required to cover a curve is used in the box analysis [26-28] or grid-cell procedure to determine the curve's length. A gauge of the length of the line can be made by duplicating the quantity of involved squares by the size of the square. The resolution at which the length of the line is measured is actually determined by the size of the grid that has been placed over the line. The  $D_f$  value can be measured with ease from this method by the following formula:

$$\text{Log } N = \alpha + \beta \text{ log } (1/s)$$

Where 's' is the dimension of the grid cells and 'N' is the number of cells counted. As it is evident from the formula that it appears to bear the equation of a straight line where  $\alpha$  and  $\beta$  are constants and the slope of the straight line, respectively. The product of 'N' and 's' gives the estimate of the perimeter length. The fractal dimension ( $D_f$ ) for the grid-cell procedure is given by the addition of the slope of the regression of  $\log \{N \times s\}$  on  $\log (1/s)$  by 1.

As the box size decreases, the length of the fractal curves also increases exponentially. In this study, the  $D_f$  values of the suture lines were measured using this method.

According to [25], the step-line process and the box approach yield different coefficients of determination ( $r^2$ ) values for the least-squares regression of length measurements vs. step-size or box size. As a result, this value is typically larger when the first method is applied; since box data tend to scatter more about the regression line, making it more difficult to determine the fractal dimension of relatively simple ammonite sutures. Due to Checa and Garcia-Ruiz's [26] demonstration that small upsides of the estimating unit provide information about the range of scale showing Euclidean way of behaving, the incline of this portion of the relapse line relating bend length to box size is consequently

somewhat diminished, while for large box-measures the number of filled boxes will generally sway occasionally, some caution is also necessary when assessing the right  $D_f$  upsides of a bend using the case strategy.

According to Lutz and Boyajian [25], the suture sinuosity index is essentially a type of fractal index with measurements at only two length scales: the ratio of the external suture length to the whorl circumference (i.e., the suture perimeter of the digitized suture/Euclidean distance between the endpoints of the suture). For truly fractal bends, such as the majority of complicated ammonoid sutures, the resolution powers of the sinuosity measure and the fractal dimension are identical at greater complexities. However, the fractal dimension has better resolution at lower complexity since it measures length at several scales. The Whorl Expansion Rate is measured by the following formula:

Whorl Expansion Rate (WER) = Whorl Diameter (W)/Whorl Diameter (W)-Apertural Height (AH). The whorl expansion rate gives an insight into the shell geometry (Fig. 6) to know about the degree of involution of a shell. Sutures of specimens analyzed in the present work were digitized by tracing them

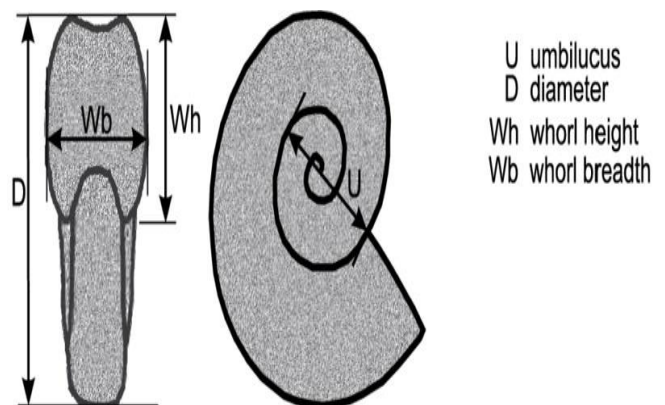


Fig. 6: Ammonite shell geometry with dimension parameters.

out from their images, with proper scale. Grids measuring 1 sq. mm, 4 sq. mm, 16 sq. mm and 36 sq. mm were placed respectively on the traced-out curves and the number of boxes were counted. The  $D_f$  values were obtained from the data

Table 1: Table showing the Raupian Parameters for three specimens, two of *Reineckeia tyranniformis* and one of *Nothocephalites paradoxus*.

Specimen No. and species name	Whorl Diameter W	Apertural height AH	W-AH	W/(W-AH)	WER
DGC/2013/J/65 <i>R. tyranniformis</i>	18.548	5.1422	13.4058	1.3835802	1.914294
DGC/2013/J/142 <i>R. tyranniformis</i>	18.25	5.8437	12.4063	1.4710268	2.16392
DGC/2013/J/148 <i>N. paradoxus</i>	10.07	3.7	6.37	1.5808477	2.49908

acquired by plotting the curve of  $\text{Log}(\text{NXs})$  over  $\text{Log}(\mathbf{1/s})$ . The  $D_f$  is calculated by the addition of 1 to the value of the slope of the regression line obtained.

#### 4. Data Analysis

Mainly 14 specimens, belonging to three broad genera, have been studied. The mean  $D_f$  value obtained was of the order of 1.444 with the maximum and minimum counts of 1.607 and 1.283 respectively.

##### 4.1 Structural Features

###### 4.1.1 Coiling

Most of the specimens studied, featured evolute coiling of shell only 1 specimen showed an intermediate coiling. The intermediately coiled specimen comprised a value of  $D_f = 1.478$  which is less than the  $D_f$  values obtained for the evolute shells (1.570), suggesting that the latter required strengthening (Table 2,4; Figs. 8-10). According to Oloriz et. al. [1] the  $D_f$  values are related to the surface-to-volume ratio (S:V), i.e., the sutural complexity depends on the surface-to-volume ratio of the camera of an ammonite shell. This has also been proved by the calculation of Whorl Expansion Rate (WER) (Table 1), suggesting that shells that are relatively involute have higher WER (2.49908) than shells with evolute coiling (1.914294).

###### 4.1.2 Whorl section

In the present study, it has been observed that the ammonite genera which have compressed high oval whorl

cross sections have greater  $D_f$  (1.607 for Eucyclocerats) values than those which have oval or sub circular whorl cross sections (1.522 for Reineckeins). This is also an indication regarding the surface-to-volume ratio of camera, which is lowest for sub-circular whorl cross sections and highest for more compressed high oval whorl cross sections [1].

##### 4.2 Ornamental Features

Evidence from the present study suggests that ammonites with medium-sized ribs have higher  $D_f$  values than ammonites with large sized ribs. Again, shells with no or medium-sized tubercles have higher  $D_f$  values than shells having larger-sized ribs or tubercles. Since the strength of ribs and tubercles changes with ontogeny; the Reineckeins species exhibit changes in  $D_f$  value accordingly (Table 2; Figs. 7-8). The Genus *Idiocycloceras* has medium sized ribs and no tubercles, corresponding to a higher  $D_f$  value (1.607) than the specimens belonging to Genus *Reineckeia* ( $D_f = 1.483$ ), which have larger ribs and coarse tubercles (Table 2; Figs. 9). Similar changes can be observed in *Nothocephalites paradoxus* during its ontogeny (Table 3; Fig. 10).

#### 5. Bathymetry

The  $D_f$  values for specimens living on epicontinental shelves and swell regions of epiocenic fringes are similar. This indicates that there are no significant differences in the habitat depth of epicontinental and epiocenic ammonites, and that correlations between sutural complexity and bathymetry are implausible. [2].

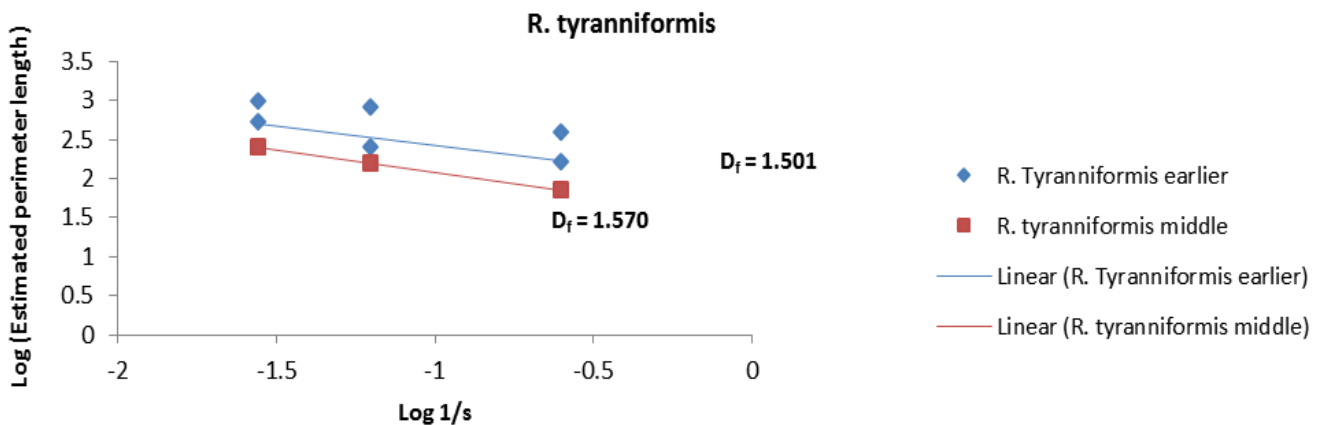


Fig. 7: Graph showing the ontogenetic variation of  $D_f$  values in *Reineckeia tyranniformis* (based on data from Table 2).

Table 2: Table showing the number of boxes counted, according to ontogeny, covering the digitized forms of suture lines, their estimated perimeter lengths, and logarithmic values for the genus *Reineckeia*. [s= Number of grid cells, N= Late growth stage, N1= Early Growth stage and N2= Middle Growth stage].

Specimen No. and species name	s	N	Ns	1/s	log (1/s)	log N	log Ns	N1	N2	N1s	N2s	log (N1s)	log(N2s)
DGC/2013/J/2	36	27	972	0.027778	-1.5563	1.431364	2.987666						
<i>R. tyranniformis</i>	16	51	816	0.0625	-1.20412	1.70757	2.91169						
	4	100	400	0.25	-0.60206	2	2.60206						
	1	197	197	1		2.294466	2.294466						
DGC/2013/J/65	36	15	540	0.027778	-1.5563	1.176091	2.732394						
<i>R. tyranniformis</i>	16	16	256	0.0625	-1.20412	1.20412	2.40824						
	4	41	164	0.25	-0.60206	1.612784	2.214844						
	1	73	73	1		1.863323	1.863323						
DGC/2013/J/142	36	7	252	0.027778	-1.5563	0.845098	2.401401	16		576		2.760422	
<i>R. tyranniformis</i>	16	10	160	0.0625	-1.20412	1	2.20412	25		400		2.60206	
	4	18	72	0.25	-0.60206	1.255273	1.857332	45		180		2.255273	
	1	40	40	1		1.60206	1.60206	83		83		1.919078	
DGC/2013/J/122	36	9	324	0.027778	-1.5563	0.954243	2.510545						
<i>R. turgida</i>	16	15	240	0.0625	-1.20412	1.176091	2.380211						
	4	43	172	0.25	-0.60206	1.633468	2.235528						
	1	89	89	1		1.94939	1.94939						
DGC/2013/J/105	36	18	648	0.027778	-1.5563	1.255273	2.811575						
<i>R. reissi</i>	16	32	512	0.0625	-1.20412	1.50515	2.70927						
	4	69	276	0.25	-0.60206	1.838849	2.440909						
	1	146	146	1		2.164353	2.164353						
DGC/2013/J/131	36	13	468	0.027778	-1.5563	1.113943	2.670246	5		180		2.255273	
<i>R. reissi</i>	16	22	352	0.0625	-1.20412	1.342423	2.546543	5		80		1.90309	
	4	41	164	0.25	-0.60206	1.612784	2.214844	16		64		1.80618	
	1	85	85	1		1.929419	1.929419	33		33		1.518514	
DGC/BHK/11	36	6	216	0.027778	-1.5563	0.778151	2.334454	4	3	144	108	2.158362	2.033424
<i>R. reissi</i>	16	10	160	0.0625	-1.20412	1	2.20412	6	4	96	64	1.982271	1.80618
	4	23	92	0.25	-0.60206	1.361728	1.963788	9	10	36	40	1.556303	1.60206
	1	48	48	1		1.681241	1.681241	18	24	18	24	1.255273	1.380211
DGC/BHK/8	36	11	396	0.027778	-1.5563	1.041393	2.597695	3	4	108	144	2.033424	2.158362
<i>R. reissi</i>	16	17	272	0.0625	-1.20412	1.230449	2.434569	4	4	64	64	1.80618	1.80618
	4	38	152	0.25	-0.60206	1.579784	2.181844	9	13	36	52	1.556303	1.716003
	1	70	70	1		1.845098	1.845098	15	25	15	25	1.176091	1.39794
DGC/2013/J/116	36	2	72	0.027778	-1.5563	0.30103	1.857332						
<i>R. reissi</i>	16	10	160	0.0625	-1.20412	1	2.20412						
	4	21	84	0.25	-0.60206	1.322219	1.924279						
	1	44	44	1		1.643453	1.643453						

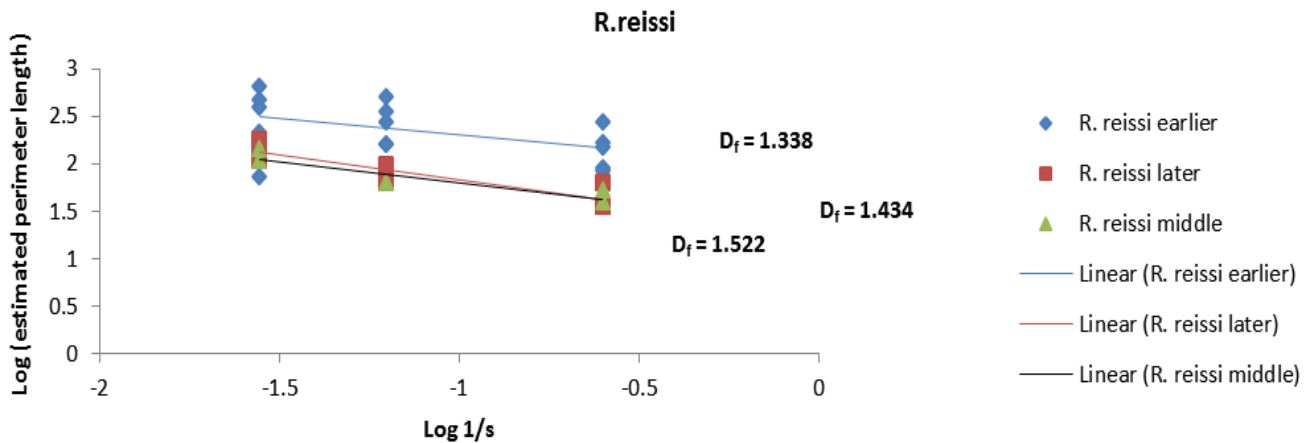


Fig. 8: Graph showing ontogenetic variation of  $D_f$  values in *Reineckeia reissi* (based on data from Table 2).

Table 3: Table showing the number of boxes counted, covering the digitized forms of suture lines, their estimated perimeter lengths, and logarithmic values for the genus *Idiocycloceras*. [s= Number of grid cells, N= Late growth stage].

Specimen No. and species name	s	N	Ns	1/s	log (1/s)	log N	log Ns
DGC/2013/137	36	17	612	0.027778	-1.5563	1.230449	2.786751
<i>I. dubium</i>	16	19	304	0.0625	-1.20412	1.278754	2.482874
	4	35	140	0.25	-0.60206	1.544068	2.146128
	1	68	68	1		1.832509	1.832509
	36	10	360	0.027778	-1.5563	1	2.556303
DGC/2013/J/78	36	10	360	0.027778	-1.5563	1	2.556303
<i>I. dubium</i>	16	14	224	0.0625	-1.20412	1.146128	2.350248
	4	25	100	0.25	-0.60206	1.39794	2
	1	50	50	1		1.69897	1.69897
	36	13	468	0.027778	-1.5563	1.113943	2.670246
DGC/2013/J/132	36	13	468	0.027778	-1.5563	1.113943	2.670246
<i>I. dubium</i>	16	16	256	0.0625	-1.20412	1.20412	2.40824
	4	32	128	0.25	-0.60206	1.50515	2.10721
	1	65	65	1		1.812913	1.812913
	36	5	180	0.027778	-1.5563	0.69897	2.255273
DGC/2013/J/134	36	5	180	0.027778	-1.5563	0.69897	2.255273
<i>I. perisphinctoides</i>	16	9	144	0.0625	-1.20412	0.954243	2.158362
	4	16	64	0.25	-0.60206	1.20412	1.80618
	1	36	36	1		1.556303	1.556303

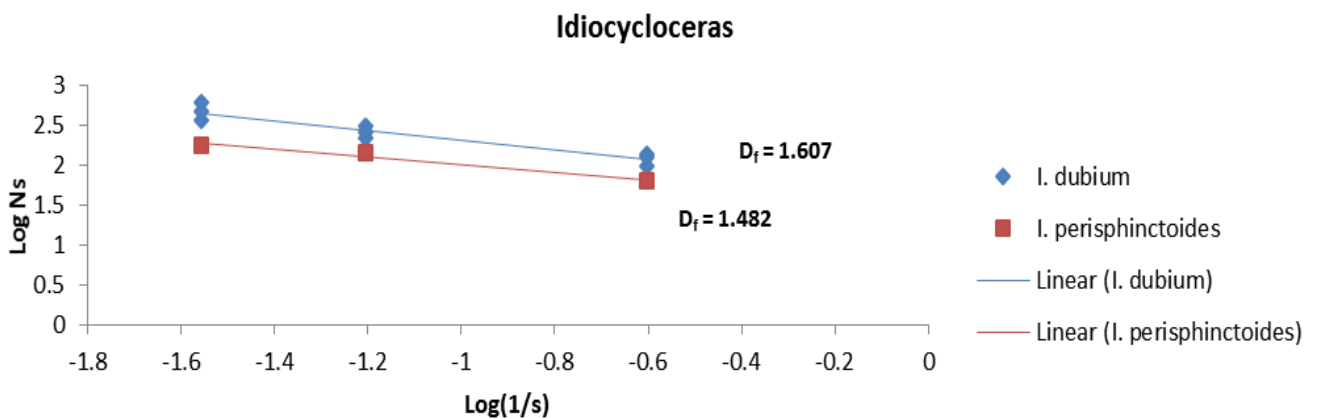


Fig. 9: Graph showing the variation in  $D_f$  values among *Idiocycloceras dubium* and *Idiocycloceras perisphinctoides* (Based on the data from Table 3).

Table 4: Table showing the number of boxes counted, according to ontogeny, covering the digitized forms of suture lines, their estimated perimeter lengths, and logarithmic values for *Nothocephalites paradoxus*. [s= Number of grid cells, N= Late growth stage, N1= Early Growth stage and N2= Middle Growth stage].

Specimen No. and species name	s	N	Ns	1/s	log (1/s)	log N	log Ns	N1	N2	N1Xs	N2Xs	log (N1s)	log (N2s)
DGC/2013/J/148	36	16	576	0.02778	-1.5563	1.20412	2.760422	2	3	72	108	1.857332	2.033424
<i>N. paradoxus</i>	16	30	480	0.0625	-1.20412	1.477121	2.681241	2	4	32	64	1.50515	1.80618
	4	52	208	0.25	-0.60206	1.716003	2.318063	7	7	28	28	1.447158	1.447158
	1	97	97	1		1.986772	1.986772	9	17	9	17	0.954243	1.230449

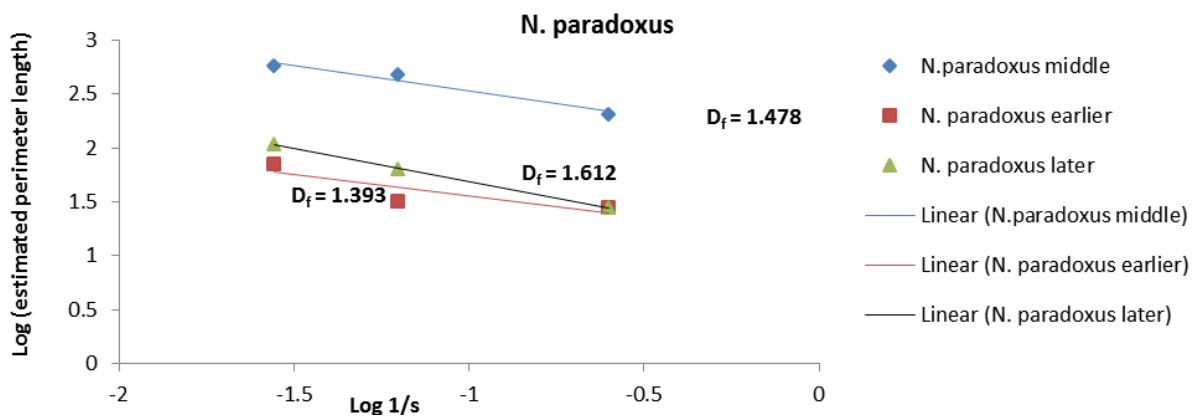


Fig. 10: Graph showing ontogenetic variation of  $D_f$  values in *Nothocephalites paradoxus* (Based on the data from Table 4).

## 6. Conclusion

Based on shell geometry, sculpture, and anticipated palaeoenvironments, fractal analysis of suture lines in Middle Jurassic ammonite groups reveals that sutural complexity was highly tied to shell traits and less so to fundamental ecology

According to some authors [29, 30], the sutural complexity is closely related to phragmocone's whorl height and degree of shell involution. In lieu of these observations presented by Pérez-Claros et al. [30], in the present study it has been observed that ammonite shells whose degree of involution is higher, has a greater  $D_f$  value than the ammonite shells with a lower degree of involution.

The present study also confirms that the complexity of suture lines is dependent on the shape of the whorl cross section i.e. highest values of  $D_f$  are seen in shells having a high oval to acute whorl cross section and the lowest values are attributed to shells with sub-circular whorl cross section. It has also been observed that shape of flanks is highly correlated with sutural complexity. Shells that are planulate have more complex sutures, hence higher  $D_f$  value, probably to accommodate a fleshy membranous bladder to become efficient in controlling the buoyancy. Moreover, the present study also unable to find any relationship between sutural complexity and bathymetry to combat shell implosion.

## Acknowledgment

The author is thankful to the Principal, Durgapur Government College for providing infrastructural and laboratory support for the research work. The author also

acknowledges financial support was provided by the DST-SERB project (CRG/2018/003717).

## References

- [1] F. Olóriz, P. Palmqvist and J.A. Pérez-Claros, "Shell features, main colonized environments, and fractal analysis of sutures in Late Jurassic ammonites," *Lethaia*, vol. 30, no. 3, pp. 191-204, 1997.
- [2] F. Olóriz and P. Palmqvist, "Sutural complexity and bathymetry in ammonites: fact or artifact", *Lethaia*, vol. 28, no. 2, pp. 167-170-204, 1995.
- [3] W.B. Saunders, "The ammonoid suture problem: relationships between shell and septum thickness and suture complexity in Paleozoic ammonoids", *Palaeobiology*, vol. 21, no. 3, pp. 343-355, 1995.
- [4] P.D. Ward, "Function of cameral water in Nautilus", *Paleobiology*, vol.6, no. 2, pp. 168-172, 1980.
- [5] S.K. Biswas, "Mesozoic Stratigraphy of Kutch, Gujarat", *Quarterly Journal of Geology Mining Metallurgical Society of India*, vol. 49, no. 3, pp. 1-52, 1977.
- [6] S.K. Biswas, "Stratigraphy and sedimentary evolution of the Mesozoic Basin of Kutch, Western India", In: S.K. Tandon, Charu C. Pant and S.M. Casshyap (Eds.), *Sedimentary Basins of India, Tectonic Context*. Gyanodaya Prakashan, Nainital, pp.74-103, 1991.
- [7] A.B. Wynne, "Memoir on the Geology of Kutch to accompany the map compiled by A.B. Wynne and F. Fedden during the sessions 1867-68 & 1868-69", *Memoires of Geological Survey of India*, vol. 9, no. 289, 1872.
- [8] Rajnath, "A contribution to the statigraphy of Kutch", *Quarterly Journal of Geology Mining Metallurgical Society of India*, vol. 4, no. 4, pp. 161-174, 1932.
- [9] K.C. Mitra, S. Bardhan and D.N. Bhattacharya, "A study of Mesozoic stratigraphy of Kutch, Gujarat with special reference to rock-stratigraphy and biostratigraphy of Keera dome", *Bulletin of Indian Geological Association*, vol. 12, no. 2, pp. 129-143, 1979.
- [10] J. Krishna, "Current Status of Jurassic stratigraphy of Kachchh, Western India", In: *International Symposium of Jurassic Stratigraphy* (Eds. O. Michelsen and A. Zeiss), vol. 3, pp. 730-741, 1984.

- [11] F.T. Fürsich and W. Oschmann, "Shell beds as tools in basin analysis: The Jurassic of Kachchh, Western India", *Journal of Geological Society of London*, vol. 150, pp. 169-185, 1993.
- [12] F.T. Fürsich, D.K. Pandey, W. Oschmann, A.K. Jaitly and I.B. Singh, "Ecology and adaptive strategies of corals in unfavourable environments: Examples from the Middle Jurassic of the Kachchh Basin, Western India", *Neues Jahrbuch für Geologie und Paläontologie – Abhandlungen*, vol. 194, no. 2-3, pp. 269-303, 1994.
- [13] N.P. Singh, "Mesozoic Lithostratigraphy of the Jaisalmer Basin, Rajasthan", *Journal of Palaeontological Society of India*, vol. 51, no. 2, pp. 1-25, 2006.
- [14] S.K. Das Gupta, "A revision of the Mesozoic-Tertiary stratigraphy of the Jaisalmer basin, Rajasthan", *Indian Journal of Earth Sciences*, vol. 2, no. 1, pp. 77-94, 1975.
- [15] D.K. Pandey, D. Kashyap and S. Choudhary, "Microfacies and depositional environment of the Gharoi River section (upper Jaisalmer Formation), west of Baisakhi Village, Jaisalmer Basin, Rajasthan", *Proceedings of the National Seminar on Oil, Gas & Lignite Scenario with Special Reference to Rajasthan*, pp. 117-130, 2005.
- [16] D.K. Pandey, J. Sha and S. Choudhary, "Depositional history of the early part of the Jurassic succession on the Rajasthan Shelf, western India", *Progress in Natural Science (Special Issue of IGCP 506 on the Jurassic Boundary Events)*, vol. 16, pp. 176-185, 2006.
- [17] D.K. Pandey, F.T. Fürsich, and M. Alberti, "Stratigraphy and palaeoenvironments of the Jurassic Rocks of the Jaisalmer Basin Field Guide", *Beringeria, Special Issue*, vol. 9, pp. 1-111, 2014.
- [18] D.K. Pandey, F.T. Fürsich and J. Sha, "Interbasinal marker intervals – A case study from the Jurassic basins of Kachchh and Jaisalmer, western India", *Science China, Series D Earth Sciences*, vol. 52, pp. 1924-1931, 2009.
- [19] H.S. Pareek, "Pre-Quaternary geology and mineral resources of northwestern Rajasthan", *Geological Survey of India, Memoirs*, vol. 115, pp. 1-99, 1984.
- [20] R.P. Kachhara and R.L. Jodhawat, "On the age of Jaisalmer Formation, Rajasthan, India", *Proceedings of IX Indian Colloquium on Micropalaeontology and Stratigraphy*, pp. 235-247, 1981.
- [21] D.K. Pandey, J. Sha, and S. Choudhary, "Sedimentary cycles in the Callovian–Oxfordian of the Jaisalmer Basin, Rajasthan, western India", *Volumina Jurassica*, vol. 8, pp. 131-162, 2010.
- [22] B.B. Mandelbrot, "The fractal geometry of nature", W. H. Freeman, New York, 1983.
- [23] G. Sugihara and R.M. May, "Nonlinear forecasting as a way of distinguishing chaos from measurement error in time series", *Nature*, vol. 344, no. 6268, pp. 734-741. doi: 10.1038/344734a0
- [24] G.E. Boyajian and T. Lutz, "Evolution of biological complexity and its relation to taxonomic longevity in the Ammonoidea", *Geology*, vol. 20, pp. 983–986, 1992.
- [25] T.M. Lutz, and G. E. Boyajian, "Fractal geometry of ammonoid sutures: Paleobiology", vol. 21, no. 3, pp. 329–342, 1995.
- [26] A.G. Checa and J. M. Garcia-Ruiz, "Morphogenesis of the septum in ammonoids," In: *Ammonoid paleobiology* (Eds. N. H. Landman, K. Tanabe and R. A. Davis), pp. 253–296, New York: Prenum, 1996.
- [27] J.M. García-Ruiz, A. Checa and P. Rivas, "On the origin of ammonoid sutures", *Paleobiology*, vol. 16, no. 3, pp. 349–354, 1990.
- [28] J.M. García-Ruiz and A.G. Checa, "A model for the morphogenesis of ammonoid septal sutures", *Geobios*, vol. 26, no. 1, pp. 157-162, 1993.
- [29] W.B. Saunders and D.M. Work, "Shell morphology and suture complexity in Upper Carboniferous ammonoids", *Paleobiology*, vol. 22, no. 2, pp. 189–218, 1996.
- [30] J.A. Pérez-Claros, F. Olóriz and P. Palmqvist, "Sutural complexity in Late Jurassic ammonites and its relationship with phragmocone size and shape: a multidimensional approach using fractal analysis", *Lethaia*, vol. 40, no. 3, pp. 253-272, 2007.